

Quantum control of a Landau-quantized two-dimensional electron gas in a GaAs quantum well using coherent terahertz pulses

T. Arikawa,^{1,2} X. Wang,^{1,2} D. J. Hilton,³ J. L. Reno,⁴ W. Pan,⁵ and J. Kono^{1,2,*}

¹*Department of Electrical and Computer Engineering, Rice University, Houston, Texas 77005, USA*

²*Department of Physics and Astronomy, Rice University, Houston, Texas 77005, USA*

³*Department of Physics, University of Alabama at Birmingham, Birmingham, Alabama 35294, USA*

⁴*Center for Integrated Nanotechnologies, Sandia National Laboratories, Albuquerque, New Mexico 87123, USA*

⁵*Sandia National Laboratories, Albuquerque, New Mexico 87123, USA*

(Received 25 September 2011; revised manuscript received 14 November 2011; published 20 December 2011)

We demonstrate coherent control of cyclotron resonance in a two-dimensional electron gas (2DEG). We use a sequence of terahertz (THz) pulses to control the amplitude of coherent cyclotron resonance oscillations in an arbitrary fashion via phase-dependent coherent interactions. We observe a self-interaction effect, where the 2DEG interacts with the THz field emitted by itself within the decoherence time, resulting in a revival and collapse of quantum coherence. These observations are accurately describable using *single-particle* optical Bloch equations, showing no signatures of electron-electron interactions, which verifies the validity of Kohn's theorem for cyclotron resonance in the coherent regime.

DOI: [10.1103/PhysRevB.84.241307](https://doi.org/10.1103/PhysRevB.84.241307)

PACS number(s): 78.67.De, 73.20.-r, 76.40.+b, 78.47.jh

Quantum coherence and many-body effects are at the heart of modern condensed-matter physics as well as solid-state quantum technologies. Since the advent of femtosecond lasers, coherent dynamics in solids have attracted much attention due to their strikingly different behaviors from those of atoms.^{1,2} These drastic differences between solids and atoms are direct consequences of many-body interactions unique to condensed matter, enhanced by other solid-state ingredients such as carrier-phonon interactions, localization, and quantum confinement. In addition, novel device possibilities such as topological quantum computation utilizing unconventional many-body properties³ have stimulated significant interest in coherent carrier dynamics in solids. Much success exists in manipulating single-particle systems such as quantum dots, whereas manipulation of many-particle quantum states has been an elusive goal.

Here, we successfully demonstrate coherent control of a two-dimensional electron gas (2DEG) in a quantizing magnetic field via cyclotron resonance, i.e., inter-Landau-level transitions. We used terahertz (THz) time-domain spectroscopy,^{4,5} which can measure the amplitude and phase of THz fields⁶⁻⁹ as well as controlling coherent dynamics using multiple pulses.¹⁰⁻¹⁴ Strikingly, our results indicate that this many-body system obeys single-particle optical Bloch equations in the weak excitation regime. We attribute this behavior to Kohn's theorem regarding the absence of many-body effects in cyclotron resonance,¹⁵ which has been proven through many continuous-wave experiments using incoherent spectroscopies.^{16,17} Our results confirm its applicability to the coherent regime, opening up new opportunities for probing and controlling coherent dynamics in quantum Hall systems.

The sample we studied contained a modulation-doped GaAs single quantum well with an electron density of $2.0 \times 10^{11} \text{ cm}^{-2}$ and a 4-K mobility of $3.7 \times 10^6 \text{ cm}^2/\text{Vs}$. Our THz magnetospectroscopy system¹⁸⁻²¹ is schematically shown in Fig. 1(a). Coherent THz pulses were generated from a nitrogen gas plasma^{22,23} created by focusing both the fundamental and second harmonic of the output of a chirped-pulse amplifier

(CPA-2001, Clark-MXR, Inc.). The first wire-grid polarizer (WGP) was placed before focusing the THz wave to the sample to make the incident wave linearly polarized along the x axis. The transmitted THz electric field through the sample was directly measured via electro-optic sampling using a (110) ZnTe crystal. To measure the y component of the transmitted THz wave, the second WGP was placed in cross-Nicole geometry before the ZnTe crystal, the [001] axis of which was perpendicular to the probe polarization (y polarized). The x component was measured by setting the second WGP parallel to the first WGP and the [001] direction of the ZnTe crystal parallel to the probe polarization. The two geometries of electro-optic sampling had the same sensitivity to the y and x components of the THz electric field, respectively, enabling quantitative comparison with each other.^{21,24} The frequency bandwidth was from 0.3 to 2.6 THz. The sample was cooled down to 1.4 K in an optical cryostat with a superconducting magnet.

Figure 1(b) shows coherent cyclotron resonance oscillations in the time domain. The left graph shows the x component of the transmitted THz field with [$E(B)$] and without [$E(0)$] a magnetic field (B) of 2 T. Small-amplitude oscillations appear after the original THz pulse when B is present. To extract the B -induced oscillations, the 0-T waveform was subtracted from the 2-T waveform, producing a decaying sinusoid with a cyclotron frequency $\omega_c/2\pi = eB/2\pi m^*$ of 0.816 THz, where e is the electronic charge, $m^* = 0.068m_0$,¹⁸ and $m_0 = 9.11 \times 10^{-31} \text{ kg}$. The inset shows the amplitude ratio between with and without B in the frequency domain, showing an absorption dip at $\omega_c/2\pi$. The right graph in Fig. 1(b) shows the y component of the transmitted THz field ($\times 10$). Again, cyclotron resonance oscillations are seen when B is present, also a sinusoid with the same cyclotron frequency, but with a different phase from the x component. The appearance of B -induced oscillations in the y component comes from the finite off-diagonal elements of the magneto-optical conductivity tensor.²⁵ Figure 1(c) shows a parametric plot of these oscillations from 7.85 to 9.05 ps, which approximately corresponds to one full period of cyclotron

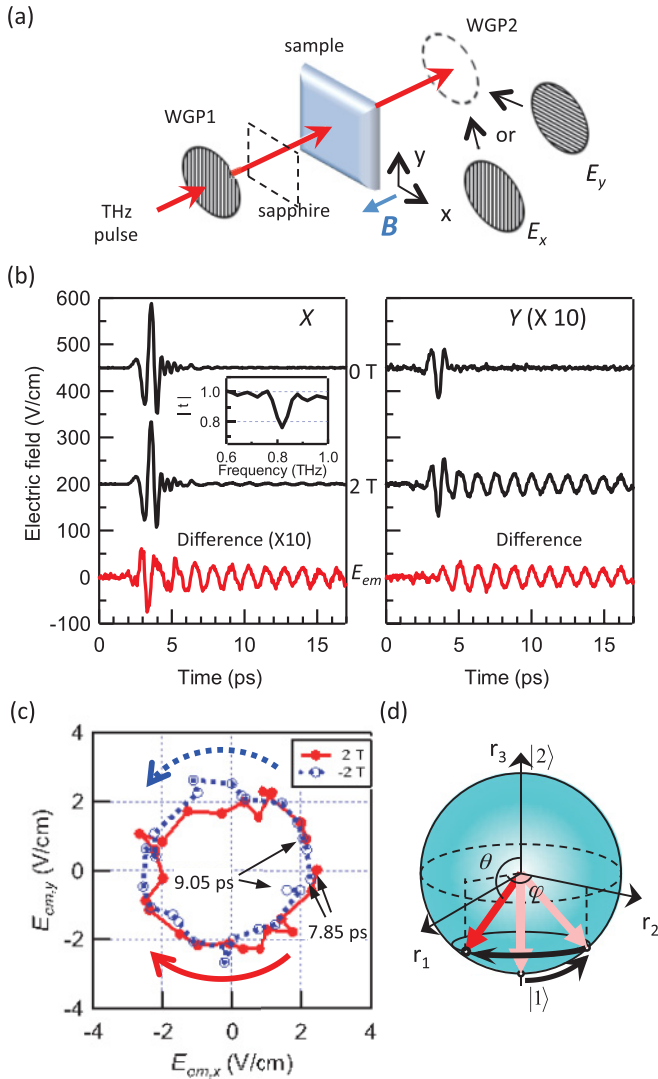


FIG. 1. (Color online) (a) Schematic of the experimental setup. WGP: wire-grid polarizer. The incident THz pulses are linearly (x) polarized. (b) Transmitted THz pulse at 0 and 2 T and the reemitted THz wave, E_{em} (x component, left and y component, right). Traces are vertically offset for clarity. Inset: amplitude ratio $|t|$ in the frequency domain showing cyclotron resonance as a dip. (c) Parametric plot showing the cyclotron resonance active mode absorption at ± 2 T. (d) Bloch sphere for coherent cyclotron resonance.

oscillation. Each point represents the tip of the electric field vector at each time, which rotates clockwise as time progresses and forms a closed circle. This shows that the absorbed THz wave is the circularly polarized cyclotron resonance active mode; the direction of rotation is reversed when the direction of B is reversed (-2 T).

Let us now turn to a quantum mechanical treatment of the observed coherent oscillations. The energy of a 2DEG in a perpendicular B is quantized into Landau levels (LLs) separated by $\hbar\omega_c$. At 2 T, the LL filling factor is 4.1, i.e., the lowest-two LLs ($|0\rangle$ and $|1\rangle$) are completely filled (including the spin degeneracy), the next level $|2\rangle$ is almost empty, and all higher levels are empty. Inter-LL transitions are allowed only between adjacent levels,^{16,17} and due to the weak THz

field employed, only a small population is excited from $|1\rangle$ to $|2\rangle$. Therefore, we treat the system as a two-level system. The incident THz pulse creates a coherent superposition $|\psi\rangle = C_1 \exp(-iE_1t/\hbar)|1\rangle + C_2 \exp(-iE_2t/\hbar)|2\rangle$, where $C_{i=1,2}$ are probability amplitudes satisfying $|C_1|^2 + |C_2|^2 = 1$. Alternatively, $|\psi\rangle$ can be expressed as a Bloch vector using coordinates (θ, φ) as $|\psi\rangle = \sin(\theta/2)|1\rangle + e^{i\varphi} \cos(\theta/2)|2\rangle$ [see Fig. 1(d)]. When the system is initially in the ground state ($|1\rangle$), the tip of the vector is at $(\theta, \varphi) = (\pi, \text{undefined})$. The tip will move to $(\theta, \varphi) = (\theta_1, 0)$ by a unitary rotation about the r_1 axis through coherent interaction with the incident THz pulse. The change in the polar angle $\pi - \theta_1$ is equal to the THz pulse area and is small (around 0.1 degrees) in our experiments. After that, the Bloch vector starts rotating at frequency ω_c , acquiring a dynamical phase $\varphi(t)$. It has an oscillating dipole moment $\langle \mu \rangle = 2\mu_{12} \text{Re}[C_1^* C_2 \exp(-i\omega_c t)]$, which reemits a THz wave E_{em} at ω_c . Here, $\mu_{12} = \langle 1|\hat{\mu}|2\rangle$ is the dipole matrix element between the states $|1\rangle$ and $|2\rangle$. In this picture, cyclotron resonance is the destructive interference of the incident field $E(0)$ and the reemitted field E_{em} , i.e., $E(B) = E(0) + E_{em}$. Thus, the B -induced oscillations [bottom traces in Fig. 1(b)] are the reemitted THz wave $E_{em} = E(B) - E(0)$ due to the induced THz dipole.

Next, we demonstrate coherent control of cyclotron resonance using a sequence of two THz pulses. Figure 2(a) shows incident pulses $E(0)$ (upper) and the y component of the reemitted field (lower) at several magnetic fields. After the second pulse is incident, reemission is quenched at 2.05 and 2.325 T, whereas reemission is enhanced at 2.175 and 2.45 T. The difference between these two cases is the oscillation phase at the arrival time t_2 of the second pulse. At 2.05 T, the sinusoid starting from 3.6 ps exhibits 7.5 periods by t_2 , i.e., the phase is an odd-integer multiple of π ; in this case, reemission is quenched. In contrast, at 2.175 T where reemission is enhanced, there are eight periods, i.e., the phase is an even-integer multiple of π . The same is true for 2.325 and 2.45 T. These situations are again understandable using the Bloch sphere [Fig. 2(b)]. In the quenching case, the phase of an odd-integer multiple of π at t_2 means that the Bloch vector is at (θ_1, π) and the rotation operation about the r_1 axis by the second THz pulse moves the vector back to $|1\rangle$ [Fig. 2(b), lower]. In the enhancement case, at t_2 the Bloch vector is at $(\theta_1, 0)$, and the rotation operation further increases θ .

Coherent dynamics of two-level atoms are describable through the optical Bloch equations.^{26,27} We applied this theoretical framework to the response of the many-electron 2DEG simply by treating the system as a collection of independent two-level systems (i.e., neglecting electron-electron interactions).²¹ The right graphs in Fig. 2(b) show the time evolution of the density matrix for 2.05 T (lower) and 2.175 T (upper), corresponding to the quenching and enhancing cases, respectively. At 2.05 T, the upper state population ρ_{22} increases through interaction with the first pulse (absorption), but decreases through interaction with the second pulse (stimulated emission). As expected, the population ρ_{22} is small due to the weak THz pulses we employed, and only the beginning of Rabi oscillations is seen. The coherence ρ_{21} is also decreased by the second pulse. In contrast, at 2.175 T, both the population and coherence are increased by the second pulse. The calculated reemitted waves are plotted in Fig. 2(a)

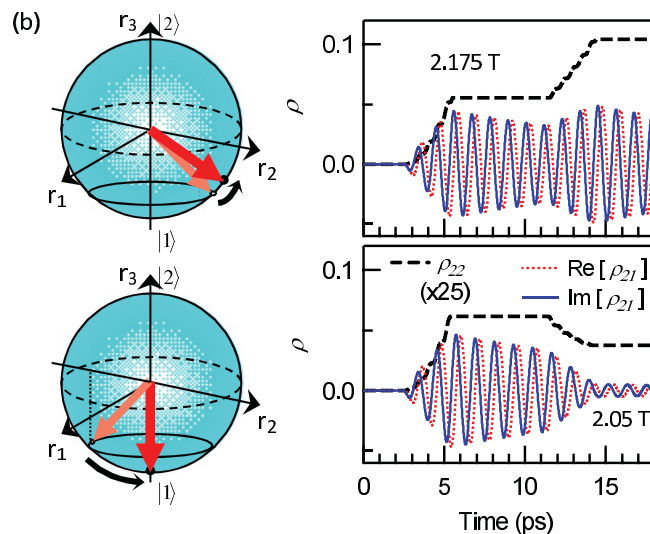
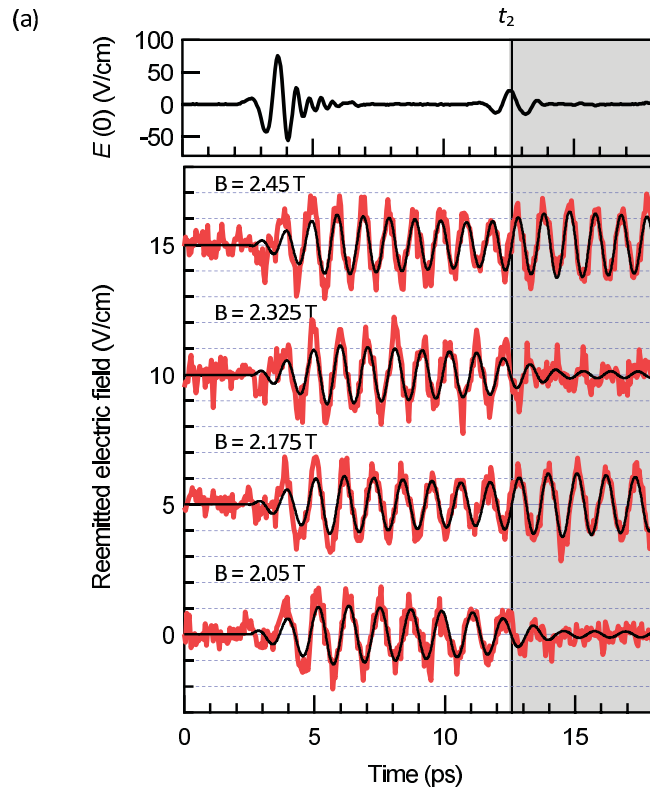


FIG. 2. (Color online) Coherent control of cyclotron resonance. (a) Incident (upper) and reemitted field (lower) at several magnetic fields. The second pulse was created through the internal reflection inside a 430- μm -thick sapphire plate [Fig. 1(a)]. (b) Bloch vector dynamics and calculated density matrix elements.

(solid black curves), reproducing the experimental data well. There are no adjustable fitting parameters in these simulations (see Supplemental Material²¹).

Finally, we describe an unusual situation where the 2DEG interacts with the THz field emitted by itself within the decoherence time [Fig. 3(a)]. This coherent “self-interaction” resulted in a revival and collapse of quantum coherence. Figure 3(b) shows a reemitted THz wave recorded for a longer time (without any intentionally created second pulse).

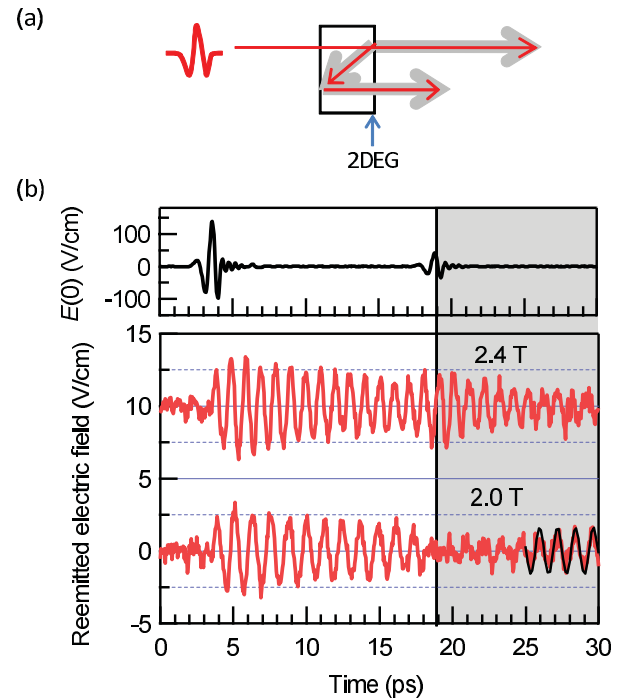


FIG. 3. (Color online) (a) The interaction of the 2DEG with its self-reemitted wave. Thick gray arrows: reemitted THz wave from the 2DEG; thin red arrows: reflected and transmitted incident THz pulse. (b) The incident electric field (upper) and reemitted field (lower). The second incident THz pulse is due to the internal reflection inside the sample substrate. The solid black curve is an extended fitting curve to the initial oscillation from 5 to 17 ps with a sine wave.

The THz pulse reflected back to the substrate by the 2DEG acquires trailing oscillations due to the backward cyclotron resonance reemission by the 2DEG [similar to the transmitted THz wave shown in the middle trace of Fig. 1(b)]. This THz pulse is further reflected by the back surface of the substrate and incident *again* onto the 2DEG at 19 ps (still less than the decoherence time). As a result, at 2 T, the amplitude of reemission, once quenched by the incident reflection THz pulse, grows again with time because of the interaction with the long-lasting self-reemitted coherent THz wave. Note that the revived oscillation is in phase with the original one in this case (blue dashed curve). In contrast, at 2.4 T, the reemission oscillations, initially enhanced by the reflection THz pulse, decay quickly due to interaction with the self-reemitted coherent THz wave. The difference between the two cases comes from the same mechanism discussed above, i.e., π difference in the arrival phase, which is again described well via optical Bloch equations.

The agreement between experiment and theory highlights the striking fact that a Landau-quantized 2DEG in a weak coherent THz field behaves in exactly the same manner as a two-level atom in a coherent radiation field. We interpret this behavior as a result of Kohn’s theorem¹⁵ regarding the absence of an influence of electron-electron interactions on cyclotron resonance frequencies. However, it is important to note that our results obtained through a coherent time-domain method reveal more about coherent cyclotron resonance dynamics than what Kohn’s theorem predicts. Namely, our

results show that not only the cyclotron resonance frequency, but also the nonequilibrium dynamical response of a 2DEG under multiple-pulse irradiation is not affected by electron-electron interactions. This result thereby broadens the realm of applicability of Kohn's theorem.

It should be also noted that at low temperatures where phonons are suppressed, the cyclotron resonance dephasing mechanism is not understood. Defects might ultimately limit the decoherence time as in dc transport (momentum relaxation time ~ 143 ps in our sample). The dephasing of *interband* photoexcited carriers (for which Kohn's theorem does not apply) is strongly dependent on the filling factor, presumably due to the electron-electron interactions within a Landau level.^{28,29} In contrast, in the present *in-traband* excitation experiments, no obvious filling-factor dependence was observed, which implies that dephasing due to electron-electron interactions is also prohibited by Kohn's theorem.

In summary, using time-domain THz techniques, we performed quantum control experiments on cyclotron resonance in a high-mobility 2DEG. We used single-particle optical Bloch equations to successfully simulate our experimental data, highlighting the striking fact that an interacting

many-electron state behaves as a single particle (Kohn's theorem for cyclotron resonance). However, the current experiments were performed in the weak excitation regime: the THz field strengths used were far from what is needed to cause Rabi oscillations. A strong THz wave would excite electrons through equally spaced higher-energy LLs in a cascading fashion, invalidating the two-level approximation. Nonparabolic systems such as InAs or graphene with nonequidistance LLs together with a narrow-band THz wave can be used to circumvent this problem.

We thank A. Belyanin and A. Imambekov for valuable discussions. This work was supported by the Sandia National Laboratories (Award No. 896506), the National Science Foundation (Grants No. OISE-0530220, No. OISE-0968405, and No. DMR-1006663), the Texas Higher Education Coordinating Board (Award No. 01905), and the Division of Materials Sciences and Engineering, Office of Basic Energy Sciences, US Department of Energy (Award No. 896506 at Sandia National Laboratories). This work was also performed in part at the US Department of Energy, Center for Integrated Nanotechnologies at Sandia National Laboratories (Contract No. DE-AC04-94AL85000).

*Corresponding author: kono@rice.edu

¹D. S. Chemla and J. Shah, *Nature (London)* **411**, 549 (2001).

²V. M. Axt and T. Kuhn, *Rep. Prog. Phys.* **67**, 433 (2004).

³S. Das Sarma, M. Freedman, and C. Nayak, *Phys. Rev. Lett.* **94**, 166802 (2005).

⁴*Sensing with Terahertz Radiation*, edited by D. Mittleman (Springer, Berlin, 2002).

⁵M. Tonouchi, *Nat. Photonics* **1**, 97 (2007).

⁶R. Kersting, R. Bratschitsch, G. Strasser, K. Unterrainer, and J. N. Heyman, *Opt. Lett.* **25**, 272 (2000).

⁷C. W. Luo, K. Reimann, M. Woerner, T. Elsaesser, R. Hey, and K. H. Ploog, *Phys. Rev. Lett.* **92**, 047402 (2004).

⁸J. Kröll, J. Darmo, S. S. Dhillon, X. Marcadet, M. Calligaro, C. Sirtori, and K. Unterrainer, *Nature (London)* **449**, 698 (2007).

⁹G. Günter, A. A. Anappara, J. Hees, A. Sell, G. Biasiol, L. Sorba, S. De Liberato, C. Ciuti, A. Tredicucci, A. Leitenstorfer *et al.*, *Nature (London)* **458**, 178 (2009).

¹⁰P. G. Hugard, J. A. Cluff, C. J. Shaw, S. R. Andrews, E. H. Linfield, and D. A. Ritchie, *Appl. Phys. Lett.* **71**, 2647 (1997).

¹¹B. E. Cole, J. B. Williams, B. T. King, M. S. Sherwin, and C. R. Stanley, *Nature (London)* **410**, 60 (2001).

¹²R. Yano, K. Nakagawa, and H. Shinojima, *Jpn. J. Appl. Phys.* **48**, 022401 (2009).

¹³T. Kampfrath, A. Sell, G. Klatt, A. Pashkin, S. Mährlein, T. Dekorsy, M. Wolf, M. Fiebig, A. Leitenstorfer, and R. Huber, *Nat. Photonics* **5**, 31 (2010).

¹⁴M. Wagner, M. Helm, M. S. Sherwin, and D. Stehr, *Appl. Phys. Lett.* **99**, 131109 (2011).

¹⁵W. Kohn, *Phys. Rev.* **123**, 1242 (1961).

¹⁶B. D. McCombe and R. J. Wagner, in *Advances in Electronics and Electron Physics*, edited by L. Marton (Academic, New York, 1975), Vol. 37, pp. 1–78.

¹⁷J. Kono, in *Methods in Materials Research*, edited by E. N. Kaufmann, R. Abbaschian, A. Bocarsly, C.-L. Chien, D. Dollimore, B. Doyle, A. Goldman, R. Gronsky, S. Pearton, and J. Sanchez (Wiley, New York, 2001), Chap. 9b.2.

¹⁸X. Wang, D. J. Hilton, L. Ren, D. M. Mittleman, J. Kono, and J. L. Reno, *Opt. Lett.* **32**, 1845 (2007).

¹⁹X. Wang, A. A. Belyanin, S. A. Crooker, D. M. Mittleman, and J. Kono, *Nat. Phys.* **6**, 126 (2010).

²⁰X. Wang, D. J. Hilton, J. L. Reno, D. M. Mittleman, and J. Kono, *Opt. Express* **18**, 12354 (2010).

²¹See Supplemental Material at <http://link.aps.org/supplemental/10.1103/PhysRevB.84.241307> for details of the experimental and theoretical methods used.

²²M. D. Thomson, M. Kreß, T. Löffler, and H. G. Roskos, *Laser Photonics Rev.* **1**, 349 (2007).

²³N. Karpowicz, X. Lu, and X.-C. Zhang, *J. Mod. Opt.* **56** (2009).

²⁴P. C. M. Planken, H.-K. Nienhuys, H. J. Bakker, and T. Wenckebach, *J. Opt. Soc. Am. B* **18**, 313 (2001).

²⁵E. D. Palik and J. K. Furdyna, *Rep. Prog. Phys.* **33**, 1193 (1970).

²⁶*Optical Resonance and Two-level Atoms* (Dover, New York, 1987).

²⁷R. W. Boyd, *Nonlinear Optics* (Academic, New York, 2008).

²⁸M. E. Karadimitriou, E. G. Kavousanaki, I. E. Perakis, and K. M. Dani, *Phys. Rev. B* **82**, 165313 (2010).

²⁹K. B. Broocks, B. Su, P. Schröter, C. H. Heyn, D. Heitmann, W. Wegscheider, V. M. Apalkov, T. Chakraborty, I. E. Perakis, and C. Schüller, *Phys. Status Solidi B* **245**, 321 (2008).